Riekki, T. S.; Sebedash, A. P.; Tuoriniemi, J. T.

Thermodynamics of adiabatic melting of solid He 4 in liquid He 3

Published in:
Physical Review B

DOI:
10.1103/PhysRevB.99.054502

Published: 05/02/2019

Document Version
Publisher's PDF, also known as Version of record

Please cite the original version:
Riekki, T. S., Sebedash, A. P., & Tuoriniemi, J. T. (2019). Thermodynamics of adiabatic melting of solid He 4 in liquid He 3. Physical Review B, 99(5), 1-8. [054502]. https://doi.org/10.1103/PhysRevB.99.054502

Thermodynamics of adiabatic melting of solid ^{4}He in liquid ^{3}He

T. S. Riekki*
Aalto University, School of Science, Low temperature laboratory, P.O. BOX 15100 FI-00076 AALTO, Finland

A. P. Sebedash
P. L. Kapitza Institute for Physical Problems RAS, Kosygina 2, 119334 Moscow, Russia

J. T. Tuoriniemi
Aalto University, School of Science, Low temperature laboratory P.O. BOX 15100 FI-00076 AALTO, Finland

(Received 18 December 2018; published 5 February 2019)

In the cooling concept by adiabatic melting, solid ^{4}He is converted to liquid and mixed with ^{3}He to produce cooling power directly in the liquid phase. This method overcomes the thermal boundary resistance that conventionally limits the lowest available temperatures in the helium fluids and hence makes it possible to reach for the temperatures significantly below 100 μK. In this paper we focus on the thermodynamics of the melting process, and examine the factors affecting the lowest temperatures achievable. We show that the amount of ^{3}He−^{4}He mixture in the initial state, before the melting, can substantially lift the final temperature, as its normal Fermi fluid entropy will remain relatively large compared to the entropy of superfluid ^{3}He. We present the collection of formulas and parameters to work out the thermodynamics of the process at very low temperatures, study the heat capacity and entropy of the system with different liquid ^{3}He, mixture, and solid ^{4}He contents, and use them to estimate the lowest temperatures achievable by the melting process, as well as compare our calculations to the experimental saturated ^{3}He−^{4}He mixture crystallization pressure data. Realistic expectations in the execution of the actual experiment are considered. Further, we study the cooling power of the process, and find the coefficient connecting the melting rate of solid ^{4}He to the dilution rate of ^{3}He.

DOI: 10.1103/PhysRevB.99.054502

I. INTRODUCTION

One of the persistent great problems in the field of low-temperature physics is the search for superfluidity of ^{3}He diluted by ^{4}He. Superfluidity of pure ^{4}He was discovered in the late 1930s [1,2] at around 2 K, but the superfluidity of pure ^{3}He was observed not until three decades later, at three orders of magnitude lower temperature [3,4]. To achieve that, completely new cooling methods had to be developed. In the quest for superfluidity of ^{3}He in ^{3}He−^{4}He mixture, we are in a similar situation: We have exhausted the search space available using the present cooling techniques, and hence a new approach is needed. The target temperatures are below 100 μK, where a BCS-type superfluid transition is expected to occur between weakly interacting ^{3}He atoms in the isotope mixture [5–8]. Such a system would be a unique dense double-superfluid ensemble consisting of fermionic ^{3}He and bosonic ^{4}He superfluids. In sparse ultracold atomic gases, this kind of mixture superfluid phase has already been observed [9,10].

Adiabatic melting of solid ^{4}He followed by its mixing with ^{3}He is one novel cooling technique proposed to achieve this temperature range. The major advantage of the method is that it bypasses the rapidly increasing thermal boundary resistance that limits the lowest temperatures available with external cooling methods, such as adiabatic nuclear demagnetization. Even as the walls of a helium container can be cooled to tens of microkelvins range, the liquid inside will remain at an elevated temperature due to the poor thermal coupling across the thermal boundary resistance bottleneck. No matter how small the heat load to the liquid is, the cooling power across the bottleneck will struggle to overcome it when temperature is low enough. The lowest directly measured temperature in ^{3}He−^{4}He mixture was 97 μK reported by Oh *et al.* [11], achieved in an experimental volume with about 4000 m^2 surface area cooled by a two-stage nuclear demagnetization cryostat.

Since the cooling by adiabatic melting takes place directly in liquid helium, the thermal boundary resistance is no longer the main factor limiting the final temperature. In this technique, first, a system of solid ^{4}He and liquid ^{3}He is precooled to as low temperature as possible with an external cooling method. Then, as the solid is melted, it releases liquid ^{4}He which will be mixed with ^{3}He producing cooling due to the latent heat of mixing. The principle of operation is somewhat similar to a conventional dilution refrigerator, the difference being that the adiabatic melting method is not continuous, and takes place at an elevated pressure [12–14].

The realization of the adiabatic melting experiment is quite a technical challenge [13]. In this paper, however, we focus on the thermodynamic aspects: The success of the melting process depends on the initial conditions and the proper execution. The final temperature ultimately achievable by this method is determined by the initial contents of the

*tapio.riekki@aalto.fi

experimental cell, which should have as little entropy as possible to begin with. An ideal initial state would contain only solid pure ^{4}He, which has negligibly small entropy, and pure superfluid ^{3}He. Below the superfluid transition temperature, its entropy decreases exponentially with temperature, so that even a small reduction in the starting temperature can significantly diminish the entropy content of the total system. In actual cases, however, there is always some ^{3}He−^{4}He mixture present, and already in quite small quantities its contribution easily dominates the total initial entropy.

We begin this paper by presenting the formulas and parameters to calculate the heat capacity and entropy of the pure ^{3}He–mixture–solid ^{4}He-system at ^{4}He crystallization pressure, and then we examine the final temperatures that can be reached with different starting conditions. A figure of merit is the cooling factor, i.e., the ratio between the initial and the final temperature. We will also discuss the cooling power due to the melting/mixing process, which is proportional to the phase transfer rate of ^{3}He, which, in turn, is related to the rate at which the ^{4}He crystal is melted. Finally, we will compare the temperature dependence of the crystallization pressure deduced from our calculations to the experimentally obtained values.

II. HEAT CAPACITY AND ENTROPY

We concentrate on the low-temperature properties (mostly below 10 mK) of phase-separated ^{3}He−^{4}He mixture at its crystallization pressure $P_C = 2.564$ MPa [15]. Our system thus consists of liquid rich and dilute ^{3}He phases, as well as solid ^{4}He phase. Under these conditions, the ^{3}He rich phase is pure ^{3}He, while the ^{3}He dilute phase contains a certain amount of ^{3}He down to the zero-temperature limit. This finite solubility is the basis of not only the conventional dilution refrigerator but also the adiabatic melting method. Superfluid ^{4}He of the mixture phase is basically in its quantum mechanical ground state and it acts as an inert background for the ^{3}He quasiparticles affecting on their effective mass [16]. Meanwhile, the solid phase can be assumed to be pure ^{4}He, provided that the crystal was grown at sufficiently low temperature ($\ll$50 mK) [17–19].

The only free thermodynamic parameter of the system is temperature T, as the solid ^{4}He phase fixes the pressure to the crystallization pressure, and the presence of the rich ^{3}He phase ensures that the dilute ^{3}He−^{4}He mixture remains at its saturation concentration $x = 8.12\%$ [20]. The system is thus a univariant three-phase system.

The Fermi systems in question, ^{3}He in the rich or dilute phase, are deep in the degenerate state so that the normal fluid heat capacity is directly proportional to the temperature $C \propto T$. At the superfluid transition temperature of the pure ^{3}He (T_c), its heat capacity suddenly increases and then drops exponentially towards lower temperatures. The isotope mixture, however, maintains the linear temperature dependence down to much lower temperatures, so that even a very small amount of ^{3}He−^{4}He mixture will eventually dominate the heat capacity of the entire system. Compared to that, we can ignore the phonon contributions to the heat capacity. This applies to all phases present, and in particular the heat capacity of the solid ^{4}He can thus be approximated as zero. Further, we assume that the molar volumes of all phases remain constant.

For the T_c of pure ^{3}He at the ^{3}He−^{4}He mixture crystallization pressure, we use the value 2.6 mK given by Pentti *et al.* [15]. This is about 10% higher than the transition temperature suggested by the provisional PLTS-2000 [21] temperature scale, but it is consistent with other characteristic ^{3}He temperatures, such as A-B and Néel transition temperatures, carefully determined at our cryostat during other experiments [22]. The precise value of the T_c is not critical to the most of the analysis presented in this paper, however, as the heat capacity and entropy can be given with respect to their value at the T_c.

The values for the parameters used in the following calculations are listed in Table I.

TABLE I. Values of the parameters used in our calculations at saturated ^{3}He−^{4}He mixture crystallization pressure. V_m, $T_{F,m}$, and $T_{F,3}$ were calculated using the other listed parameters, while A and B are fitting parameters for the pure ^{3}He heat capacity below the T_c. ‡This value was scaled due to the difference in the temperature scales between Ref. [24] and us (see text).

Parameter	Symbol	Value	Ref.
^{3}He−^{4}He mixture crystallization pressure	P_C	2.564 MPa	[15]
^{3}He Sommerfeld constant‡	γ	3.44 K^{-1}	[24]
^{3}He superfluid transition temperature	T_c	2.6 mK	[15]
^{3}He effective mass in ^{3}He−^{4}He mixture	m^*/m_3	3.32	[6]
Saturation concentration	x	8.12%	[20]
BBP-parameter	α	0.164	[29]
Liquid ^{4}He molar volume	$V_{4,l}$	23.16 cm^3/mol	[28]
Solid ^{4}He molar volume	$V_{4,s}$	20.97 cm^3/mol	[32]
Liquid ^{3}He molar volume	V_3	26.76 cm^3/mol	[31]
Liquid ^{3}He−^{4}He mixture molar volume	V_m	23.47 cm^3/mol	Eq. (5)
^{3}He−^{4}He mixture Fermi temperature	$T_{F,m}$	0.378 K	Eq. (4)
^{3}He Fermi temperature	$T_{F,3}$	1.43 K	$= \pi^2(2\gamma)^{-1}$
Superfluid ^{3}He energy gap	Δ_0	$1.91T_c$	[26], [27]
First fitting parameter	A	8.242	Eq. (3)
Second fitting parameter	B	11.22	Eq. (3)

The heat capacity for n moles of degenerate Fermi fluid is given by [23]

$$\frac{C}{nR} = \frac{\pi^2}{2}\frac{T}{T_F}, \tag{1}$$

where R is the molar gas constant, and T_F the Fermi temperature. The heat capacity of normal fluid pure ^{3}He is usually expressed with the Sommerfeld constant $\gamma = \pi^2(2T_F)^{-1}$ as

$$\frac{C_3(T > T_c)}{n_3 R} = \gamma T, \tag{2}$$

where n_3 is the amount of ^{3}He in the pure phase. By interpolating the data given by Greywall [24], we can find $4.14\,\mathrm{K}^{-1}$ for the γ-parameter at the P_C. But the temperature scales used by Greywall and us differ by about 10%, as manifested by the different superfluid transition temperature values used by us ($T_c = 2.6\,\mathrm{mK}$) and Greywall ($T_{c,\mathrm{Gw}} = 2.37\,\mathrm{mK}$). Now, since $\gamma = C/T = dQ/(T\,dT)$, we need to scale the above value by $(T_{c,\mathrm{Gw}}/T_c)^2$ to maintain consistency, giving us $\gamma = 3.44\,\mathrm{K}^{-1}$. The value obtained this way is close to the coefficient interpolated from the data by Alvesalo *et al.* [25], approximately $3.2\,\mathrm{K}^{-1}$ at the P_C. Although the about 20% margin in the γ-parameter is rather inconvenient, it is not unheard of. As already pointed out by Greywall [24], this magnitude of discrepancy in the γ-values obtained by various experimental groups can be attributed to the difference in their temperature scales.

To describe the behavior of pure ^{3}He below the superfluid transition temperature T_c with a single smooth function over the entire temperature range, we use the expression

$$\frac{C_3(T \leqslant T_c)}{n_3 R} = \gamma T_c\left[\left(\frac{A}{\widetilde{T}} + B\widetilde{T}^2\right)\exp\left(-\frac{\Delta_0}{T}\right)\right], \tag{3}$$

where $\widetilde{T} = T/T_c$ is the reduced temperature, A and B are fitting parameters, and $\Delta_0 = 1.91T_c$ is the superfluid ^{3}He energy gap at the zero-temperature limit, taken as average of the values given by Refs. [26] and [27]. The fit was made against the normalized heat capacity data by Greywall [24].

The heat capacity of ^{3}He$-^4$He mixture is given by Eq. (1), using the Fermi temperature of the mixture as [16,23]

$$T_{F,m} = \frac{\hbar^2}{2m^* k_B}\left(\frac{3\pi^2 N_A x}{V_m}\right)^{2/3}, \tag{4}$$

where $x = 8.12\%$ [20] is the saturation concentration of the mixture, and $\hbar$, k_B, and N_A are the reduced Planck constant, Boltzmann constant, and Avogadro constant, respectively. The effective mass of ^{3}He atom $m^* = 3.32m_3$ ($m_3 = 3.0160293\,u$ is the bare ^{3}He mass) was calculated using the quasiparticle interaction potential from Ref. [6] at the saturation concentration. Next, the molar volume of the mixture V_m is evaluated from [5]

$$V_\mathbf{m} = V_{4,l}(1 + \alpha x), \tag{5}$$

where $V_{4,l} = 23.16\,\mathrm{cm}^3/\mathrm{mol}$ [28] is the molar volume of liquid pure ^{4}He, and α is the BBP-parameter that describes the extra volume occupied by the lighter ^{3}He atoms with their larger zero-point motion. We use the value $\alpha = 0.164$ extrapolated from Ref. [29]. With these the mixture molar volume is $V_m = 23.47\,\mathrm{cm}^3/\mathrm{mol}$. The Fermi temperature of the mixture is thus $T_{F,m} = 0.378\,\mathrm{K}$, and the heat capacity per mole of ^{3}He in the mixture $n_{m,3}$ becomes

$$\frac{C_{m,3}}{n_{m,3}R} = 13.05\,\frac{T}{\mathrm{K}}. \tag{6}$$

In Fig. 1 we show the heat capacities for several ^{3}He/^{4}He partitions, starting from a system consisting of pure ^{3}He

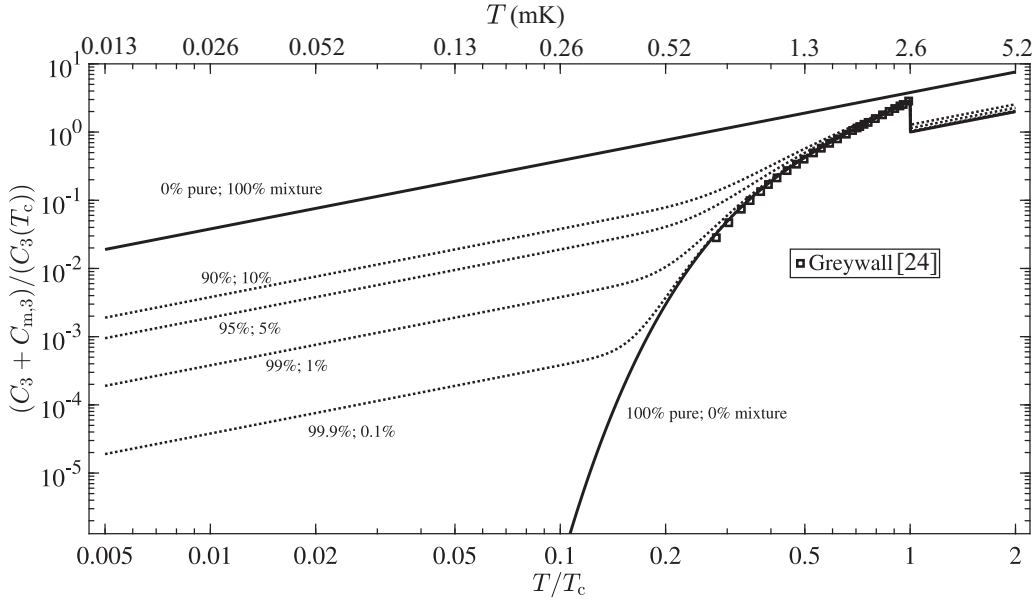

FIG. 1. Total heat capacity of pure ^{3}He (C_3), and ^{3}He$-^4$He mixture ($C_{m,3}$) system per mole of ^{3}He as a function of the temperature below $2T_c$ calculated from Eqs. (2), (3), and (6). The heat capacity values are scaled by its value at the pure ^{3}He T_c. Experimental data for pure ^{3}He by Greywall [24] are shown for comparison. The percentages tell how the total amount of ^{3}He in the system is split between pure ^{3}He phase and ^{3}He$-^4$He mixture phase.

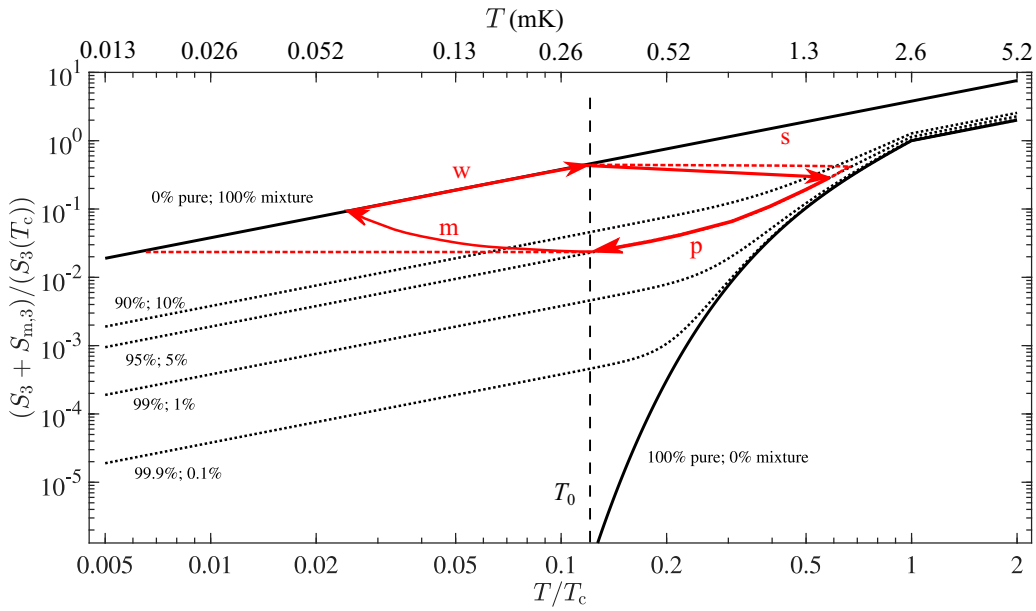

FIG. 2. Total entropy of pure ^{3}He (S_3), and ^{3}He$-^4$He mixture ($S_{m,3}$) system per mole of ^{3}He as a function of the temperature below $2T_c$. The entropy values are scaled by its value at the pure ^{3}He T_c. The red arrows indicate a solidification (s)–precooling (p)–melting (m)–warm-up (w) cycle with 5% of the total ^{3}He remaining in mixture after the solid growth, considered as quite a conservative value. The precooling temperature is indicated as T_0. The cycle was drawn assuming losses during the melting process (m) due to the heat leak to the experimental cell, while during the solidification (s) the precooling starts already as the solid is growing. The red horizontal dashed lines indicate perfectly adiabatic melting and solidification paths for comparison. The percentages tell how the total amount of ^{3}He in the system is split between pure ^{3}He phase and ^{3}He$-^4$He mixture phase.

together with solid ^{4}He, and then letting a portion of the total ^{3}He amount to be in the mixture phase so that the total ^{3}He amount of the system remains constant. Entropies of ^{3}He and mixture can then be calculated from the heat capacity as the integral $S = \int_0^T \frac{C}{T} dT'$; in the case of Eq. (3) numerical integration is required. They are shown in Fig. 2.

In an ideal, perfectly adiabatic melting process, where the pure ^{3}He phase shrinks and the mixture phase grows, one moves horizontally from right to left in diagrams like those of Figs. 1 and 2, and the final temperature will be determined by the initial conditions alone. If the initial mixture amount is vanishingly small, even minor improvements to the precooling conditions lead to a huge gain in the cooling factor, since the entropy of the pure superfluid ^{3}He phase decreases exponentially. However, in realistic cases, there is always some small amount of mixture left. Then, from Fig. 2 we see that precooling the system to below $0.15T_c$ no longer decreases the total entropy as rapidly, since even a minuscule mixture amount is enough to become the main contributor to the total entropy at those temperatures. $0.15T_c$ is quite a reasonable value for a decent precooling temperature, as it can be reached using an adiabatic nuclear demagnetization refrigerator. Figure 2 also shows an example of an operational cycle of the cooling process, which begins with the solidification of the ^{4}He crystal (s), followed by the precool along the constant pure ^{3}He–mixture content curve (p). When the set precooling temperature T_0 is reached, the melting process is initiated by removing ^{4}He from the cell (m), and at the end one reaches the mixture curve. In practice, the crystal may not always be completely melted, but as the remaining undissolved ^{3}He has only very small entropy, this will not greatly affect the final temperature. When the melting is done, the system may be allowed to warm-up back to the precooling temperature (w), after which the crystal is regrown. The cycle in Fig. 2 was drawn by assuming some losses in the melting process due to the external heat leak to the experimental cell, which we have taken to be of order $200\,\mathrm{pW/mol_{^3He}}$.

III. COOLING FACTOR

Cooling factor of the adiabatic melting process c_F is defined as the ratio between the temperatures before and after the melting, $c_F = T_0/T_{\mathrm{final}}$. Above the pure ^{3}He T_c, both the pure and the dilute phase entropy follow the linear temperature dependence, and hence the cooling factor remains constant. The optimal value for the cooling factor above the T_c can be evaluated from Eqs. (2) and (6) by assuming that the initial state contains only pure ^{3}He and solid ^{4}He, while the final state is exclusively ^{3}He$-^4$He mixture. We get $c_F(T > T_c) = \pi^2/(2\gamma T_{F,m}) \approx 3.8$. The conventional dilution refrigerators operate at low pressure with a cooling factor comparable to this.

Below the T_c, however, the potential cooling factor increases rapidly as soon as the entropy of pure ^{3}He starts to decrease exponentially. With ideal precooling conditions, with the system at that stage consisting only of solid ^{4}He and superfluid pure ^{3}He, with no mixture phase, the cooling factor can reach values up to several hundreds as the precooling temperature approaches $0.15T_c$. The presence of the mixture phase in the initial state severely limits the possible cooling factors, as shown in Fig. 3. If even 1% of the total amount of pure ^{3}He remains in the mixture at the beginning, the

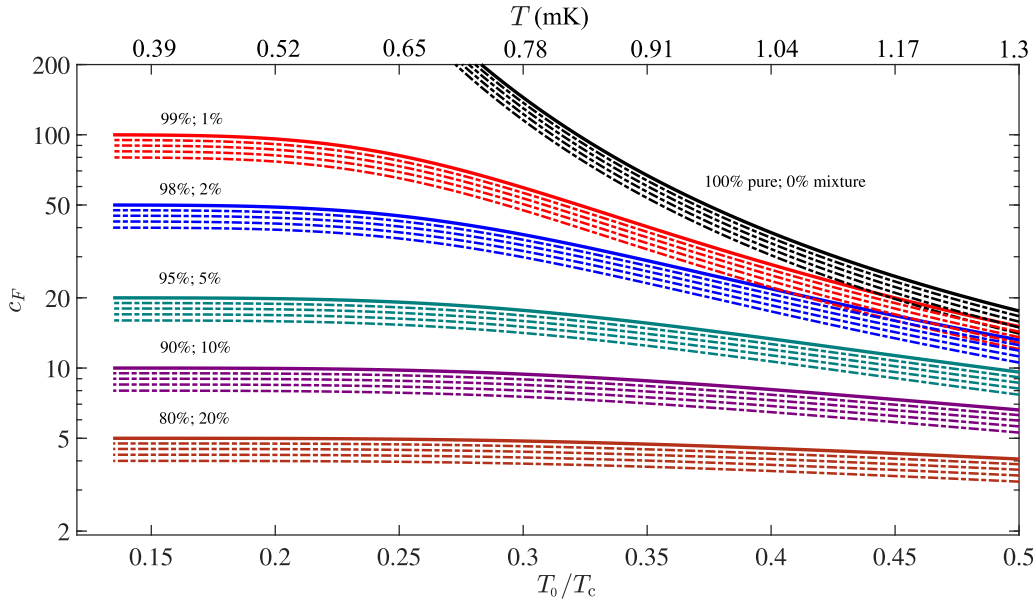

FIG. 3. Cooling factors in perfectly adiabatic melting processes, below $0.5T_c$, as a function of the precooling temperature T_0, with different starting conditions from an ideal case with no mixture phase to one where 20% of the total ^{3}He is in the mixture phase at the beginning of the melting process. The solid lines indicate the melting processes that have no pure ^{3}He left in the end, while the dash-dotted lines correspond to incomplete melting processes ending with 5%, 10%, 15%, and 20% of the total ^{3}He still in the pure ^{3}He phase.

cooling factor levels out at around 100. Further precooling will not help increase it, as the entropy of the entire system is now dominated by the entropy of the mixture phase. Of course, lower initial temperature still results in a lower final temperature, but just in proportion. With nonideal starting conditions, the upper limit for the cooling factor is determined by the ratio between the total amount of ^{3}He in the system and the amount of ^{3}He in the mixture phase $c_{\mathrm{F,max}} = (n_3 + n_{m,3})/n_{m,3}$. In conclusion, to achieve optimal cooling by the adiabatic melting method, it is essential to minimize the amount of ^{3}He$-^4$He mixture in the initial state.

Figure 3 shows not only the cooling factors in complete melting processes where the final state contains no pure ^{3}He phase, but also the cooling factors for four different incomplete meltings. The effect on the cooling factor caused by partial melting is not nearly as substantial as the presence of the initial mixture phase. From practical aspects, it is not always desirable to melt the crystal entirely to ensure easier regrowth process as no new nucleation is required. Also, the experimental cell may contain surplus of ^{3}He to accommodate separate sintered heat exchanger for the precooling stage, where the mixture with rather large viscosity is not desired to enter.

IV. COOLING POWER

The cooling power $\dot{Q}$ of the adiabatic melting process is due to the latent heat of mixing of ^{3}He from the pure phase to the mixture phase. It is given by

$$\dot{Q} = T\dot{n}_3(S_{m,3} - S_3), \tag{7}$$

where $\dot{n}_3$ is the rate at which ^{3}He is transferred between the phases, and S_3 and $S_{m,3}$ are the entropies per ^{3}He atom in the pure and the mixture phase, respectively. Well below the T_c, when the temperature is low enough for the ^{3}He$-^4$He mixture to dominate the total entropy of the system, we can ignore S_3, and the expression simplifies to

$$\dot{Q} \approx 109\,\frac{\mathrm{J}}{\mathrm{mol\,K^2}}\,\dot{n}_3 T^2. \tag{8}$$

At $T = 100\,\mu$K, and with $\dot{n}_3 = 100\,\mu$mol/s, this gives about 100 pW of cooling power. To achieve similar cooling power with an external cooling method, the surface area of the helium cell would have to be of order $10\,000\,\mathrm{m}^2$, which was estimated using the thermal boundary resistance values from Ref. [30]. Such large surface areas are hard to obtain in practice, as it would require several kilograms of sintered silver powder layered on the cell surfaces.

The cooling power depends on the rate $\dot{n}_3$, at which ^{3}He atoms transfer from the pure phase to the mixture phase. In the actual experiment, we cannot directly measure this, but rather we have control over the extraction rate of ^{4}He out from the cell ($\dot{n}_4$). To facilitate the melting process, the ^{4}He amount corresponding to the molar volume difference between the solid and liquid phases has to be removed from the cell, and vice versa if the crystal is grown. Hence, it is essential to calculate the conversion factor ϑ in $\dot{n}_3 = \vartheta\dot{n}_4$, which tells us how the extraction rate of ^{4}He corresponds to the phase transfer rate of ^{3}He. Let us denote the total volume of the experimental cell as v, and assume that it contains n_3 moles of pure ^{3}He, n_s moles of solid ^{4}He, and n_m moles of ^{3}He$-^4$He mixture, and thus

$$v = n_3 V_3 + n_s V_{4,s} + n_m V_m, \tag{9}$$

where $V_3 = 26.76\,\mathrm{cm}^3/\mathrm{mol}$ [31] is the molar volume of pure ^{3}He, and $V_{4,s} = 20.97\,\mathrm{cm}^3/\mathrm{mol}$ [32] is the molar volume

of solid ^{4}He, while V_m is as given by Eq. (5). When an infinitesimal amount of solid is melted (or grown) the contents change to

$$v = (n_3 - dn_3)V_3 + (n_s - dn_s)V_{4,s} + (n_m + dn_m)V_m. \quad (10)$$

Combining Eqs. (9) and (10), and taking the time derivative, results in

$$\dot{n}_3 V_3 + \dot{n}_s V_{4,s} - \dot{n}_m V_m = 0. \quad (11)$$

The total amount of ^{3}He in the system remains constant, which means that

$$\dot{n}_3 - x\dot{n}_m = 0, \quad (12)$$

while the amount of ^{4}He is changing by the amount required to melt the crystal, giving

$$\dot{n}_s - (1-x)\dot{n}_m = \dot{n}_4, \quad (13)$$

where $\dot{n}_4$ is the rate at which pure ^{4}He is removed from the cell. Using Eqs. (12) and (13) together with Eq. (11) yields

$$\begin{aligned} &\dot{n}_3 V_3 + \left[\dot{n}_4 + (1-x)\frac{\dot{n}_3}{x}\right]V_{4,s} - \dot{n}_3 V_m = 0 \\ \Rightarrow\ &\dot{n}_3 = \frac{xV_{4,s}}{(1+\alpha x)V_{4,l} - xV_3 - (1-x)V_{4,s}}\dot{n}_4 \\ &\equiv \vartheta \dot{n}_4. \end{aligned} \quad (14)$$

With the numerical values, that can be found from Table I, we get $\vartheta \approx (0.84 \pm 0.01)$. Using this, the low temperature cooling power of the adiabatic melting, expressed in terms of the ^{4}He extraction rate, becomes

$$\dot{Q} = 109\,\frac{\mathrm{J}}{\mathrm{mol\,K^2}}\,\vartheta \dot{n}_4 T^2 \approx 91\,\frac{\mathrm{J}}{\mathrm{mol\,K^2}}\,\dot{n}_4 T^2. \quad (15)$$

Figure 4 shows the cooling power up to 400 μmol/s extraction rates. Since there inevitably exists some background heat leak in any real experimental setup, the lowest possible temperature is reached when the cooling power matches the heat leak. Furthermore, the melting process itself may cause rate dependent dissipation due to the movement of the pure ^{3}He–mixture interface, for example. Therefore, there obviously exists an optimal melting rate which maximizes the cooling power while keeping any additional losses at sustainable level. With proper cell design the dissipative losses should not become an issue. 400 μmol/s under 100 pW load results in the equilibrium at $T \approx 0.022T_c \approx 60\,\mu$K.

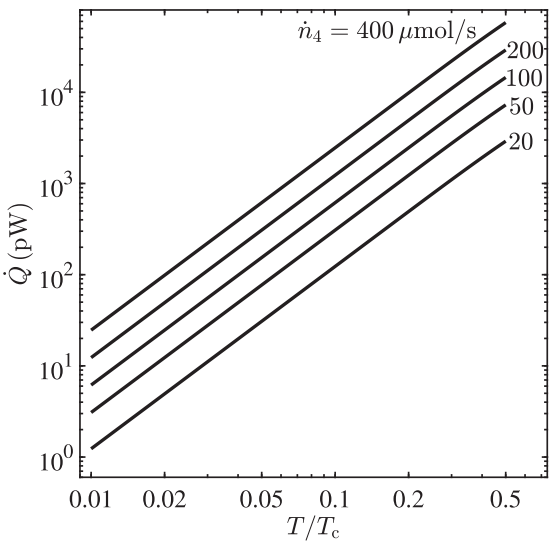

FIG. 4. Cooling power of the adiabatic melting method at different ^{4}He extraction rates $\dot{n}_4$ calculated from the entropy difference between the mixture and pure ^{3}He phases [Eq. (7)].

As a side note, another useful conversion factor is the change in the amount of solid in the cell $\dot{n}_s$, when $\dot{n}_4$ ^{4}He is added or removed. We can solve it by eliminating $\dot{n}_3$, and $\dot{n}_m$ from Eqs. (12)–(14), yielding

$$\dot{n}_s = \left[1 + \left(1 - \frac{1}{x}\right)\vartheta\right]\dot{n}_4 \approx 10.5\dot{n}_4. \quad (16)$$

This is useful in determining the amount of solid ^{4}He in the cell. Further, the denominator of Eq. (14) can be rearranged to

$$\begin{aligned} \Delta V &= (V_{4,l} - V_{4,s}) + x(\alpha V_{4,l} - V_3 + V_{4,s}) \\ &\approx (2.19 - 1.99x)\,\mathrm{cm^3/mol}, \end{aligned} \quad (17)$$

which is the change in the molar volume between solid and liquid phase in the saturated mixture. The first term is the molar volume difference between pure liquid ^{4}He and solid ^{4}He, while the second term is due to the presence of ^{3}He.

V. CRYSTALLIZATION PRESSURE

Once we have the entropies and molar volumes for all components of the system, we can work out the slope of the crystallization pressure as the function of temperature through the Clausius-Clapeyron relation $dP_\mathrm{C}/dT = \Delta S/\Delta V$. This is a directly measurable quantity. Both at the zero-temperature limit and above the T_c up to about 50 mK this is directly proportional to temperature, so that the derivative of P_C with respect to T^2 is expected to be constant at these regimes.

Above the T_c, the quadratic crystallization pressure coefficient is given by [15]

$$\begin{aligned} \left.\frac{dP_\mathrm{C}}{d(T^2)}\right|_{T>T_c} &= \frac{x(S_{m,3} - S_3)}{2\Delta V} \\ &= \frac{x\pi^2 R}{4\Delta V}\left(\frac{1}{T_{F,m}} - \frac{1}{T_{F,3}}\right), \end{aligned} \quad (18)$$

where ΔV is given by Eq. (17), and $T_{F,m}$ and $T_{F,3} = \pi^2(2\gamma)^{-1}$ are the mixture and the pure ^{3}He Fermi temperatures, respectively. At the zero-temperature limit (effectively when $T \lesssim 0.2T_c$), this reduces to [15]

$$\left.\frac{dP_\mathrm{C}}{d(T^2)}\right|_{T\to 0} = \frac{xS_{m,3}}{2\Delta V} = \frac{x\pi^2 R}{4\Delta V T_{F,m}}, \quad (19)$$

as $S_3 \ll S_{m,3}$. The ratio of the coefficients between the two regimes is then $(1 - T_{F,m}/T_{F,3})^{-1}$, which assumes the numerical value 1.36 with our choice of parameters (Table I).

There are experimental data on these coefficients at different temperature intervals in Refs. [15], [33], and [34]. Pentti *et al.* [15] give data within a limited temperature range both below and above the T_c and quote the values 0.92 Pa(mK)$^{-2}$ above the T_c and 1.52 Pa (mK)$^{-2}$ at the zero-temperature limit, resulting in a ratio 1.65 between the two.

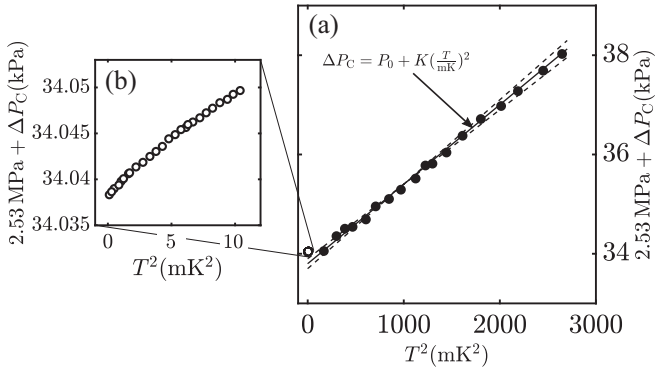

FIG. 5. Difference of the crystallization pressure ΔP_C from the pure ^{4}He zero-temperature value (2.530 MPa) as a function of T^2. (a) The data points are the experimental data by Salmela *et al.* [33] (•) and Pentti *et al.* [15] (○), while the solid line is a fit to the (•) data with $K = dP_C/d(T^2) = (1.6 \pm 0.1)\,\mathrm{Pa\,(mK)^{-2}}$ and $P_0 = (33.8 \pm 0.1)\,\mathrm{kPa}$. The dashed lines indicate the confidence bounds of the fit. (b) Close-up of the crystallization pressure data by Pentti *et al.* [15].

Salmela *et al.* [33] give data in the normal state up to about 50 mK. However, they present fitted values for the quadratic coefficients only at constant concentrations below saturation (thus on crucially different two-phase systems), but the paper also gives data on the saturated system as discrete points. Performing a similar fit upon these data gives the quadratic coefficient $(1.6 \pm 0.1)\,\mathrm{Pa\,(mK)^{-2}}$, represented in Fig. 5. This result is in perfect agreement with the corresponding value $dP_C/d(T^2) = 1.60\,\mathrm{Pa(mK)^{-2}}$ calculated with Eq. (18) using the parameters at Table I [below the T_c with Eq. (19) we get $2.17\,\mathrm{Pa\,(mK)^{-2}}$]. This result thus supports the validity of our adopted parameter values. In particular, our choice for the $T_c = 2.6$ mK at the mixture crystallization pressure, the overall temperature scale, and the suggested scaling for the normal state heat capacity coefficient γ of pure ^{3}He get some backing from this. Without scaling the Greywall's [24] γ value, the above T_c slope would become $1.48\,\mathrm{Pa\,(mK)^{-2}}$, which is also off from the value determined by Pentti *et al.* [15] [$0.92\,\mathrm{Pa(mK)^{-2}}$].

Yet another set of data can be found from Ref. [34], whose measurements extend beyond the domain of validity of the quadratic temperature dependence. These authors give the quadratic coefficient as $1.285\,\mathrm{Pa(mK)^{-2}}$ and find it necessary to amend the description by a quartic term $-2.065\,\mathrm{MPa(mK)^{-4}}$, good from 60 to 140 mK. The deviation from the quadratic behavior is caused in part by the increase in the liquid mixture saturation concentration when the temperature rises, by the molar volumes departing from their constant values, but most importantly by the fact that ^{3}He begins to dissolve into the solid phase as well at that range of temperatures. The extremely neat quadratic behavior of $P_C(T)$ below 50 mK demonstrates that the solid phase is indeed free from dissolved ^{3}He there.

The inconveniently broad range of the quadratic coefficients above the T_c indicated by these works is, of course, somewhat disconcerting. The measurements of Refs. [33] and [15] utilized differential pressure gauges with extremely good sensitivity, but the measurements of Ref. [15] may have suffered from the effect of rather small reference volume, as discussed in Ref. [35]. This deficit was improved by the measurements in Ref. [33]. Also, the temperature span covered in Ref. [15] was rather limited and the quoted value for the saturation concentration 7.3% is questionable. No good reason for the discrepancy between the measurements in Refs. [33] and [34] can be given, except that the necessity to include the quartic term in the fit of Ref. [34] may have introduced some bias towards the quadratic term as well. The conclusion must be that the genuine values for these parameters at very low temperatures are not yet as well established as one might wish.

VI. CONCLUSIONS

Growing the solid phase into a helium mixture at low temperature can result in a complete phase-separation into solid ^{4}He and liquid ^{3}He. Adiabatic melting of such solid ^{4}He, and its following mixing with liquid ^{3}He is a cooling method that can be used in attempts to reach sub-100 μK temperatures in superfluid ^{3}He and saturated ^{3}He−^{4}He mixture at its crystallization pressure. The ability to reach the lowest possible temperature is strongly dependent on the mixture content of the experimental volume before the melting process is initiated: Relative to pure superfluid ^{3}He, ^{3}He−^{4}He mixture carries a large amount of entropy, and therefore its presence in the initial state can significantly limit the final temperature. The ideal initial state would contain only solid ^{4}He and pure ^{3}He, and since below the T_c, the pure ^{3}He entropy will decrease exponentially, the total entropy content of the system drops rapidly enabling reduction in temperature ideally by several orders of magnitude.

The question regarding the practical execution of the experiment is how to minimize the amount of the initial state mixture. If the mixture amount is determined by some intrinsic property of the setup, such as geometry disrupting the growth of the solid, or porous structures (e.g., sinter) trapping the mixture phase, one cannot reduce it below some threshold value. Another question is whether it is safe to assume that there are no ^{3}He inclusions in the solid phase. Such ^{3}He bubbles in the crystal would remain hotter than the bulk liquid during the precooling process, and while melting one should then be able to observe sudden heating spikes caused by the release of these inclusions. This can obviously be avoided by proper growing conditions [17] and is not expected to be a serious issue.

Another crucial point is to determine where the heat leak to the experimental cell is coming from, and how to minimize it. Some of it is coming from the precooling stage through the thermal boundary resistance bottleneck, since the liquid is cooled to a lower temperature than the cell structures at the melting period. Measurements themselves contribute to this and the connecting capillaries are bound to conduct heat from the hotter parts of the cryostat. Since one can never completely get rid of the heat leak, an obvious question is, what is the optimal melting rate of the solid under the given conditions. The heat leak would have the least effect on the final temperature if the melting was done as quickly as possible, limited by the critical velocity in the ^{4}He extraction line, or the time

needed for performing the necessary measurements. But if there are some dissipative losses related to the movement of the pure ^{3}He–mixture-interface, then there may exist possibly lower optimum value. These questions will be addressed in the future, once our running experiment has produced sufficient amount of data to enable such analysis.

ACKNOWLEDGMENTS

The authors thank J. Rysti for insightful discussions. This work was supported by the Jenny and Antti Wihuri Foundation Grant No. 00170320, and it utilized the facilities provided by Aalto University at OtaNano, Low Temperature Laboratory infrastructure.

[1] P. Kapitza, Nature **141**, 74 (1938).
[2] J. F. Allen and A. D. Misener, Nature **142**, 643 (1938).
[3] D. D. Osheroff, R. C. Richardson, and D. M. Lee, Phys. Rev. Lett. **28**, 885 (1972).
[4] D. D. Osheroff, W. J. Gully, R. C. Richardson, and D. M. Lee, Phys. Rev. Lett. **29**, 920 (1972).
[5] J. Bardeen, G. Baym, and D. Pines, Phys. Rev. **156**, 207 (1967).
[6] J. Rysti, J. T. Tuoriniemi, and A. J. Salmela, Phys. Rev. B **85**, 134529 (2012).
[7] M. K. Al-Sugheir, H. B. Ghassib, and B. R. Joudeh, Int. J. Mod. Phys. B **20**, 2491 (2006).
[8] A. Sandouqa, B. Joudeh, M. Al-Sugheir, and H. Ghassib, Acta Phys. Pol. A **119**, 807 (2011).
[9] I. Ferrier-Barbut, M. Delehaye, S. Laurent, A. T. Grier, M. Pierce, B. S. Rem, F. Chevy, and C. Salomon, Science **345**, 1035 (2014).
[10] R. Roy, A. Green, R. Bowler, and S. Gupta, Phys. Rev. Lett. **118**, 055301 (2017).
[11] G. H. Oh, Y. Ishimoto, T. Kawae, M. Nakagawa, O. Ishikawa, T. Hata, T. Kodama, and S. Ikehata, J. Low Temp. Phys. **95**, 525 (1994).
[12] A. P. Sebedash, J. T. Tuoriniemi, S. T. Boldarev, E. M. M. Pentti, and A. J. Salmela, J. Low Temp. Phys. **148**, 725 (2007).
[13] A. Sebedash, S. Boldarev, T. Riekki, and J. Tuoriniemi, J. Low Temp. Phys **187**, 588 (2017).
[14] A. P. Sebedash, JETP Lett. **65**, 276 (1997).
[15] E. Pentti, J. Tuoriniemi, A. Salmela, and A. Sebedash, J. Low Temp. Phys. **146**, 71 (2007).
[16] E. R. Dobbs, *Helium Three*, International Series of Monographs on Physics (Oxford University Press, Oxford, 2001).
[17] C. Pantalei, X. Rojas, D. O. Edwards, H. J. Maris, and S. Balibar, J. Low Temp. Phys. **159**, 452 (2010).
[18] S. Balibar, T. Mizusaki, and Y. Sasaki, J. Low Temp. Phys. **120**, 293 (2000).
[19] S. Balibar, J. Low Temp. Phys. **129**, 363 (2002).
[20] E. M. Pentti, J. T. Tuoriniemi, A. J. Salmela, and A. P. Sebedash, Phys. Rev. B **78**, 064509 (2008).
[21] R. L. Rusby, M. Durieux, A. L. Reesink, R. P. Hudson, G. Schuster, M. Kühne, W. E. Fogle, R. J. Soulen, and E. D. Adams, J. Low Temp. Phys. **126**, 633 (2002).
[22] M. S. Manninen, A. Ranni, J. Rysti, I. A. Todoshchenko, and J. T. Tuoriniemi, J. Low Temp. Phys. **183**, 399 (2016).
[23] E. Lifshitz and L. P. Pitaevskii, *Statistical Physics: Theory of the Condensed State (Pt 2)* (Butterworth-Heinemann, London, 1980).
[24] D. S. Greywall, Phys. Rev. B **33**, 7520 (1986).
[25] T. A. Alvesalo, T. Haavasoja, and M. T. Manninen, J. Low Temp. Phys. **45**, 373 (1981).
[26] I. A. Todoschenko, H. Alles, A. Babkin, A. Y. Parshin, and V. Tsepelin, J. Low Temp. Phys. **126**, 1449 (2002).
[27] J. Serene and D. Rainer, Phys. Rep. **101**, 221 (1983).
[28] E. Tanaka, K. Hatakeyama, S. Noma, and T. Satoh, Cryogenics **40**, 365 (2000).
[29] G. E. Watson, J. D. Reppy, and R. C. Richardson, Phys. Rev. **188**, 384 (1969).
[30] A. P. J. Voncken, D. Riese, L. P. Roobol, R. Konig, and F. Pobell, J. Low Temp. Phys. **105**, 93 (1996).
[31] M. Kollar and D. Vollhardt, Phys. Rev. B **61**, 15347 (2000).
[32] A. Driessen, E. van der Poll, and I. F. Silvera, Phys. Rev. B **33**, 3269 (1986).
[33] A. Salmela, A. Sebedash, J. Rysti, E. Pentti, and J. Tuoriniemi, Phys. Rev. B **83**, 134510 (2011).
[34] J. Rysti, M. S. Manninen, and J. Tuoriniemi, J. Low Temp. Phys. **175**, 739 (2014).
[35] A. Sebedash, J. T. Tuoriniemi, S. Boldarev, E. M. Pentti, and A. J. Salmela, in *24th International Conference on Low Temperature Physics - LT24*, edited by Y. Takano, S. P. Hershfield, S. O. Hill, P. J. Hirschfeld, and A. M. Goldman, AIP Conf. Proc. No. 850 (AIP, New York, 2006), p. 1591